Towards Net Zero Energy Factory: a multi-objective approach to optimally size and operate industrial flexibility solutions

L. Bartolucci[a], S. Cordiner[a], V. Mulone[a], M. Santarelli*[,a] P. Lombardi[b], B. Arendarski[b]
[a] University of Rome Tor Vergata, via del Politecnico 1, 00133, Rome, Italy
[b] Fraunhofer Institute for Factory Operation and Automation IFF, Sandtorstraße 22, 39106, Magdeburg, Germany

Abstract

This study proposes a methodology for sizing and operating new flexibility options within a German carpentry, targeting to be operated as Net Zero Energy Factory (NZEF). A key element of this system is the maximization of the integration of the electric power locally generated by a photovoltaic plant and the electric demand for driving the manufacturing processes. This aim is achieved with a proper integration between design of flexibility options and optimal control of energy flows. In this work, benefits and criticalities arising from the integration of different flexibility options, such as stationary and mobile Energy Storage Systems, are identified and analyzed.

A double step optimization process is implemented. First, a Model Predictive Control strategy is used to schedule the manufacturing machines and the energy storage systems (stationary and mobile). Then, a multi-objective optimization aiming at the minimization of annual energy grid exchange and the optimal exploitation of battery capacity is carried out with the Genetic Algorithm. Such a methodology allows the factory operators to optimally size the flexibility capacity (the battery energy storage in this application) needed to operate their industrial facility a net-zero energy factory.

Results show that an optimally controlled stationary energy storage system allows a reduction of grid energy exchange up to 53%. The further introduction of electric vehicles increases of about 5% and 67% the renewable energy self-consumption and carbon emissions savings, respectively, ensuring also a significant increase in the yearly annual savings (up to 406%).

***Keywords*— Energy Storage System, Net-Zero-Energy-Factory, Model Predictive Control, Multi-objective Optimization, Electric Vehicles**

NOMENCLATURE

1

α_1	wight associated to energy grid exchange objective
α_2	weight associated to BESS exploitation objective
BESS	Battery Energy Storage System
C_{BESS}	BESS Capacity [kWh]
C_{EV}	Electriv Vehicle battery capacity [kWh]
δ_{comp}	load compression factor
δ_{BESSch}	binary variable for charging BESS
$\delta_{BESSdch}$	binary variable for discharging BESS
δ_{EVch}	binary variable for charging EV
δ_{EVdch}	binary variable for discharging EV
δ^{i}_{idle}	binary variable for idle machine
δ^{i}_{on}	binary variable for ON/OFF machine
D_{BESS}	Distance from Optimal Technical solution
DOD_{cycle}	Depth of Discharge of BESS cycle [%]
E_{BESS}	Energy throughout the BESS [kWh]
E_{GRID}	Energy exchange with grid [kWh]
EMS	Energy Management System
e_{travel}	emission factor of thermal vehicles [$kgCO_2$/km]
EV	Electric Vehicle
GWP_{GRID}	Global Warming Potential of the grid [$kgCO_2/kWh_{consumed}$]

GWP_{BESS}	Global Warming Potential of BESS [$kgCO_2/kWh_{installed}$]
$I_{sizeBESS}$	BESS exploitation Index [%]
I_{SC}	Self-Consumption Index [%]
k	time constant
L_{cycle}	BESS life in cycles
$life_{BESS}$	BESS life [years]
MILP	Mixed Integer Linear Porgramming
MPC	Model Predictive Control
NDS	Non dominated Sorting
NSGA II	Non Sorted Genetic Algorithm
NZEF	Net Zero Energy Factory
N_{cycles}	Number of BESS cycles
p	Rate of production
P_{buy}	Power bought from the grid [kW]
P_{sell}	Power sold to the grid [kW]
P_{BESSch}	Power Charge of BESS [kW]
$P_{BESSdch}$	Power Discharge of BESS [kW]
P_{load}	Power demand of load [kW]
P_{PV}	Power Production from PV [kW]
P^{i}_{on}	Power demand in ON state of machine i [kW]
$\mathrm{P}^{\mathrm{i}}_{\mathrm{idle}}$	Power demand in idle state of machine i [kW]
$\mathrm{P}^{\mathrm{nom}}_{\mathrm{comp}}$	Peak Power demand of compressor [kW]
P_{EVch}	Power Charge of EV [kW]
P_{EVdch}	Power Discharge of EV [kW]
PV	Photovoltaic
RES	Renewable Energy Sources
SME	Small Medium Enterprise
SOB	State of Buffer
SOC_{BESS}	State of Charge of BESS [%]
SOC_{EV}	State of Charge of EV [%]

1. Introduction

The European Union aims at increasing the share of Renewable Energy Sources (RES) to at least 32% by 2030. Member States have identified national action plans to comply with the targets enacted by EU Directives. For example, in Germany a set of policies summarized under the term Energiewende (lit. "energy transition") has been implemented with the aim to cut the 80% of the greenhouse gases before 2050 and have a nuclear-free energy supply by 2022 [1]. These goals have been targeted by reducing the primary energy consumption and increasing the renewable energy share to 80% of the gross final energy demand.

The industrial sector has given a great contribution to reach such goals. Indeed, in 2017 about 14% of the small and medium enterprises used predominantly renewable energy and around the 22 % planned to do it in the following 2 years (Figure 1). The largest increases have been observed amongst SMEs in Germany (+22 %), Italy (+18 %) and Austria (+18 %) [2]. However, in many cases, the electric energy generated has not been directly integrated into the enterprise electric network but has been first fed into the grid and then drawn to cover the manufacturing loads. This is the so-called "feed and forget approach", giving issues for the compensation to be acted by grid operators. In many European countries, the feed and forget approach has been allowed for 20 years starting from the installation of PV plants and many system operators have suggested that, at the expiration of that period, the PV operators should pay to feed the grid.

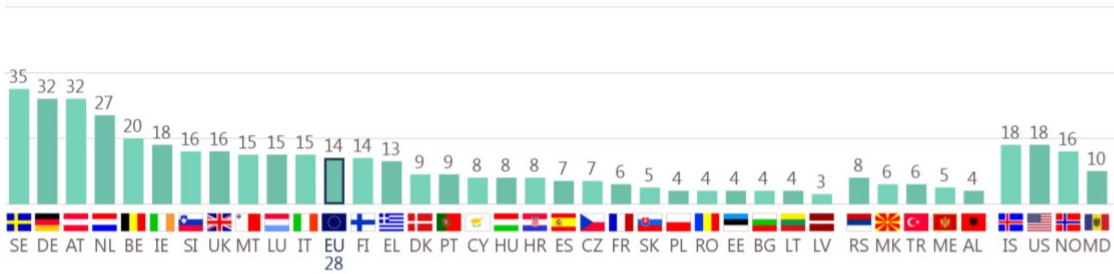

Figure 1 - Percentage of Small and Medium Enterprises using predominantly renewable energy (e.g. including own production through solar panels) - Base: All SMEs (N=12,907) [1]

Therefore, higher RES penetration necessarily entails a radical transformation of the current energy system in order not to affect the reliability of services and increase the energy cost for the users. Energy Storage Systems (ESS) represent one of the most analyzed options [3]. However, such solution might require huge amount of economic, space and material resources [4]. Considering as an example Germany, if only ESS were considered for compensating the volatility of renewable energy sources, about 43TWh of new storage capacity would be required [5]. A more sustainable solution is represented by local RES balancing within a micro-grid framework [6]–[8].

In the specific case of the industrial sector, the maximization of the self-consumption throughout the increase of the manufacturing process flexibility and storage capability has become a key feature. In this regard, EU has been supporting several projects for different energy intensive companies [9][10]. Among these, there are some focusing on the possibility to transform factories into Net Zero Energy Factory (NZEF) as a possible solution to avoid the network overfeeding in five to ten years and increase the sustainability of this sector. Within this framework, the main contribution of this study lies on developing a methodology to design and plan the needed flexibility options allowing to operate the manufacturing factories as NZEF. A German carpentry has been considered as a case study. On the roof of the carpentry a photovoltaic plant able to generate up to 126 kW of electric power is installed. The suggested methodology aims at both exploiting the hidden flexibility of the manufacturing processes and to size energy storage systems (stationary and mobile) for operating the industrial facility as a net-zero energy factory. The suggested methodology might be adopted by industrial users for sizing the capacity of storage solutions to improve the flexibility which could not be derived by the manufacturing processes. Moreover, the developed methodology considers other aspects (i.e. the logistic) that are not directly connected to the production system, but that hides flexibility potential to operate industrial facilities as net-zero energy systems.

The study is structured as following: in section 2 a literature review on the concept of Net Zero Energy Factory and the exploitation of its flexibilities is described. In section 3 a study case related to the identification, design and planning of new flexibility options within a German carpentry is explained. Section 4 is dedicated to the introduction of the optimal battery sizing strategy and the results are presented in Section 5. Section 6 comes up summarizing the major conclusions of the work.

2. Net Zero Energy Factory concept and flexibility exploitation

In the last years, the concept of Net Zero Energy System (NZES) has captured more and more the attention of the scientific community, but its definition is still ambiguous and involves different elements [11]. However, a NZES is commonly defined as a system in which the annual electricity consumption equals to its annual electricity generation [12]. In most of the analyzed cases, this framework is referred either to residential and commercial buildings [13]–[18] or to larger systems, like quarters, cities and villages [19], [20]. In the last years, this concept has been widely applied to the industrial sector too, so that it is possible to refer to the industrial enterprises whose yearly consumption is largely covered by RES production as Net Zero Energy Factory (NZEF). This is the case of some large industrial companies, like Tesla or Mitsubishi [21], [22]. Thus, in a general way, a NZEF could be classified as an industrial microgrid [23], in which the electric power is also locally generated using volatile RES, having a specific primary aim: minimizing the net energy grid exchange throughout the exploitation of its flexibility options and the increase of renewable self-consumption. Operating industrial facilities as NZEF allows better integrating the electric power generation by volatile renewable energy sources (like wind and sun) into the grid. Indeed, by reducing the feeding of volatile RES generation into the grid, the operative costs that the system operators must face for balancing the intermittent generation decrease as well. Moreover, balancing the volatile RES fluctuations locally allows reducing also grid infrastructure upgrading costs required for increasing the RES penetration into the energy sector. With such a perspective, designing and operating of industrial facility as net-zero energy systems have a positive consequence on the decarbonization process toward an energy scenario 100% renewable based.

One of the main characteristics of the NZEF is the presence of a metering digital infrastructure able to evaluate data and supply predictions to automatic control processes or workers, so that they might adjust the manufacturing process accordingly. The core element of this infrastructure is the Energy Management System (EMS), whose control logic can be based on mathematical models, multi-agent models [24], [25] or machine learnings algorithms [26]. In literature, several works described EMS used for day-ahead scheduling and real-time control with the main aim to minimize the operational and/or the environmental costs. Generally, both economic and emission related objectives have been pursued rescheduling the operation of one or more workstations so that the plant operation has been reduced during peak-load hours, when the price of electricity is higher [27]–[29], and/or has been shifted in time to exploit the availability of on-site generation from renewables [30], [31]. Authors in [32] achieved an annual cost saving of 28.1% with respect to a reference case by optimizing the manufacturing scheduling of a hybrid grid-connected factory under a Time-Of-Use tariff scheme. Yu et al. in [33] showed how it is possible to have a reduction up to 23.5% of the operative costs when Demand Response program are deployed in face of ever-changing real-time prices. In [34], instead, a multi-objective optimization considering as decision variables the penetration rate of process equipment and technologies has been implemented. In [35], a holistic approach to plan a data center as a net-zero energy system has been proposed, showing how planning industrial or tertiary facilities as multi-energy systems might allow to increase the integration of RES volatility into the industrial processes.

In the aforementioned works, economic savings have mainly been achieved adapting the load consumption to the energy prices or RES production rather than trying to reduce the net grid energy exchange. In this work, instead, the optimal industrial process scheduling has been implemented considering the net zero energy goal as the main objective.

Regardless of the system extension, when there is a significant RES production, a key element to reach such target is the integration of extra new flexibility options, like storage devices [36]–[38] in a multi-energy-system framework [39]–[41]. To this end, a comprehensive technical knowledge of all the energy-intensive processes in a factory is crucial [42]. In [43] a methodology based on usage of smart meters has been suggested for identifying, quantifying and exploiting flexibilities within a job-shop process operated as net-zero energy factory. In [44] Bartolucci et al. show how seasonal hydrogen storage can allow achieving an almost self-independence (up to 85%) in the case of a university building.

In literature, benefits from the introduction of buffer stocks, compressed air storage reservoirs, electric and thermal energy storage systems have already been considered [45], [46], but the problem of optimally sizing the ESS in industrial frameworks has not been explored in detail yet. Indeed, there are several papers addressing the problem of optimal battery sizing for Net Zero Energy buildings, but most of the time are residential ones [11], [15], [17]. Facci et al. [47] studied a possible solution to promote positive synergy between local PV production, heating operation and thermal energy storage achieving up to 41% and 73% reduction respectively in energy costs and carbon emissions. The identification of the most effective flexibility sources within the industrial context is more challenging with respect to the residential case, due to the higher complexity and variability of the manufacturing process constraints. Indeed, the requirements and standards vary a lot according to sector and size of the system.

Thus, the main contribution and objective of this study is to apply a robust optimization to a much more complex system using a consolidated and well-known sizing methodology for battery energy storage system (BESS). Moreover, differently from the aforementioned papers, in this work the NZEF boundaries have been extended from the production process to the logistics, substituting the conventional thermal vehicles with Electric Vehicles (EVs). To the best of the authors knowledge, there are no studies in literature evaluating the potential of the EVs to achieve the net zero energy target and evaluating the effectiveness of their presence from a technical, economic and environmental point of view, when another flexibility source has to be sized. Indeed, Pham et al. in [48] did not take into account as decision variables their charging process in the optimization, or authors in [49], [50] treated EVs as extra storage devices in a Vehicle-To-Grid approach but not with the aim to reduce the net energy exchange between the factory and the grid. This work is aimed to fill this gap.

A last important consideration concerns how the introduction of different flexibility sources could have both positive and negative impacts in a system. As demonstrated in [14], they could contribute to positively improve the supply and demand matching only if properly sized and controlled through an efficient EMS. Authors in [18] also pointed out that a system economic performance would differ significantly between optimal and non-optimal operation strategies and, thus, the optimal operation solution should be used to identify the proper system design. In this study, a Model Predictive Control (MPC) approach has been chosen, on the basis of the successful results obtained in managing the thermal and electric load to provide ancillary services [51]–[53] and reducing the energy storage system sizing [54]–[56]. This control strategy has been widely adopted for residential and tertiary buildings but only few works have exploited its potential for industrial applications [57], [58]. Thus, as a further element of novelty of this work, a MPC strategy has been implemented to optimally plan the weekly production activity, control the battery and manage the EVs charging process with the objective to minimize the energy exchange with the grid.

By considering the all the above mentioned aspects, the main contributions of this study can be summarized as following:

- Development a methodology allowing to exploit flexibility within job-shop processes to increase the matching between local RES availability and factory demand;
- Developing an optimal scheduling strategy taking into account as decision variables both the manufacturing and the logistic linked resources (i.e. electric fleet);
- Provide a comprehensive sizing methodology for a flexibility source, specifically a battery energy storage system (BESS), with the target of achieving NZEF;
- Perform a comprehensive analysis of the synergetic effects of the optimized use of BESS and EVs when a Model Predictive Control is used in a NZEF perspective;
- Provide a decision tool to the factory operators for choosing among all the possible BESS sizes that minimize the net energy exchange with the grid the optimal one toward a technical, economic and environmental target.

3. Flexibility options identification within net zero energy factory

The system layout considered in this study is shown in Figure 2 and consists of a grid-connected carpentry with a photovoltaic (PV) plant. A stationary BESS and a fleet of EVs are considered as options to increase the flexibility degree of the manufacturing system. An inverter enables the energy exchange between the loads and the energy sources through a DC bus. It has been assumed that PV panels, BESS and the charging station have individual control systems, handling the energy exchange at the bus interface.

The energy production of the 126kW peak power PV plant has been estimated using historical data of the weather conditions collected in site (Magdeburg-Germany). In particular, the weekly irradiance is assumed to be known in advance for the optimal scheduling process.

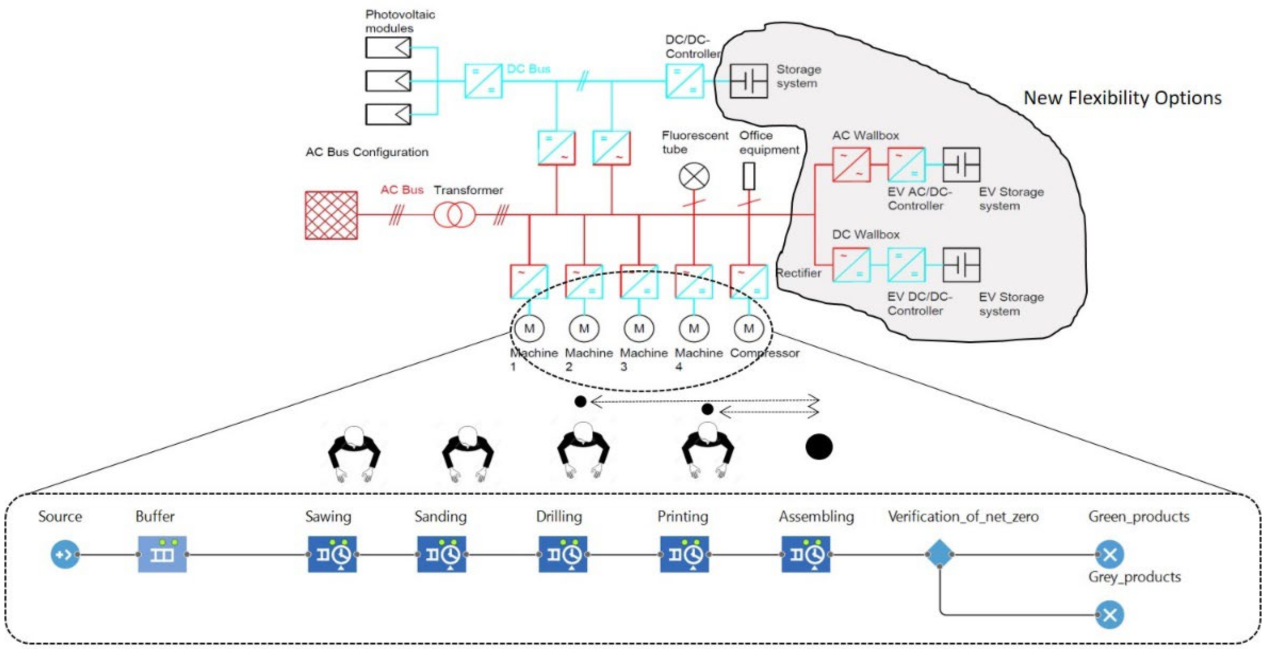

Figure 2 - System electric layout with AC grid in red and DC grid in Ciano. Below a schematic description of the manufacturing process

The electric load considered in this study is the one required by a particular manufacturing process carried out in the carpentry. It consists of a job shop process, split into five sub-processes: 1) sawing, 2) sanding, 3) drilling, 4) printing and 5) assembling. Thus, five different types of products are daily produced. The assembling sub-process requires compressed air, which is supplied by a compressor system, and to operate all the sub-processes four workers are considered. An agent-based model has been implemented to analyze the manufacturing system, from the point of view of both the electric power flow and the material flow. Figure 3 shows the PV power generation of a spring day (metered data) and a simulated load profile for manufacturing twenty goods. It is evident that most of the generated electric power does not match the manufacturing process load.

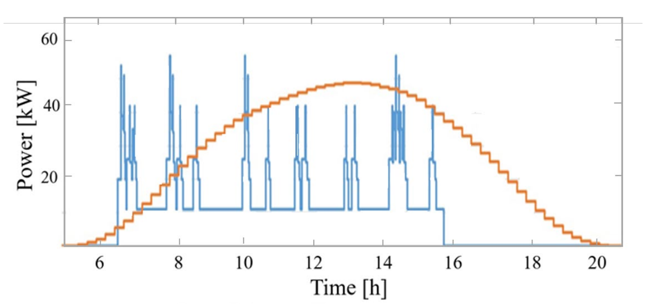

Figure 3 - Load (blue line) and generation profiles (orange line) of springy day

In order to avoid feeding the external grid and, therefore, to export volatility to the grid operator, new flexibility options have to be introduced. As first step, they should be identified and successively evaluated. In this study three different possibilities have been considered: 1) load shifting, 2) use of stationary BESS, 3) use of vehicle batteries. The last option requires the introduction into the logistic factory fleet of electric vehicles.

For job-shop processes requiring the presence of the operators, gain in flexibility through load shift might be limited by the human resources themselves as the activation of the sub-processes are manually done. However, this flexibility option might be better exploited if material buffer stocks are considered, and the daily production target is scheduled in advance. Thus, in order to evaluate the potential offered by the load shifting, buffer stocks have been introduced and the production processes has been planned through a MPC strategy. A planning horizon of one week has been chosen, and this timespan has been discretized with a time-step of 30 minutes as a compromise between model accuracy and computational complexity. Mixed-Integer Linear Programming (MILP) algorithm has been used to solve the scheduling problem. A complete mathematical description of the control strategy has been reported in a previous work [46], however, a brief description of the main aspects is recalled for the sake of clarity.

The load required by the overall production process at each time step t can be expressed as in Equation 1:

$$P_{load} = \sum_{i}^{I} (\delta_{on,t}^{i}\, P_{on,t}^{i} + \delta_{idle,t}^{i}\, P_{idle,t}^{i}) + \delta_{comp,t} P_{comp}^{nom} \tag{1}$$

where δ_{on}^{i} and δ_{idle}^{i} are two binary variables associated to each machine to distinguish between production and idle mode respectively, while the off state is expressed as a combination of the two values $\delta_{on}^{i} = 0$, $\delta_{idle}^{i} = 0$; δ_{comp} is a continuous variable describing the load factor of the compressor.

Equation 2 ensures the mutual exclusion of production and idle mode for each machine

$$\delta_{on,t}^{i} + \delta_{idle,t}^{i} \leq 1 \tag{2}$$

The filling level of any buffer stock j is represented by the integer variable SOB_t^j, whose dynamic evolution can be modelled according to Equation 3:

$$SOB_t^j = SOB_{t-1}^j + p^{i-1} - p^{i+1} \tag{3}$$

where p^{i-1} and p^{i+1} are the rates of production (number of items per time step) of the preceding and the following machine, respectively. Maximum and minimum levels are imposed for each buffer to avoid production starvation (Equation 4):

$$SOB_{min}^j \leq SOB_t^j \leq SOB_{max}^j \tag{4}$$

Benefits in terms of load and production from RES matching deriving from load shifting with respect to a standard scheduling approach are highlighted in Figure 4. In a standard scheduling the production process is organized in such a way that the most energy demanding machines (sawing and sanding machines) never work at the same time, while the others turn on whenever the previous buffers have reached a level of piece allowing continuous operation for a minimum period (see ref. [36] for further details). The MPC algorithm, instead, is able to exploit the flexibility offered by the material buffers in order to schedule the production process with the aim of minimizing the energy exchanged with the grid. This feature leads to an increase in percentage of load covered by PV, which grows in [37] from 46,2% with a standard control approach to 63,8% with the MPC strategy. However, the contribution on flexibility offered by simply load shifting and material buffer is still limited, and several practical issues could arise. For example, material buffer stocks for short-medium time storage might require a significant amount of space. Thus, to achieve the net zero energy target it emerges the need to combine different flexibilities options as the BESS (stationary and mobile).

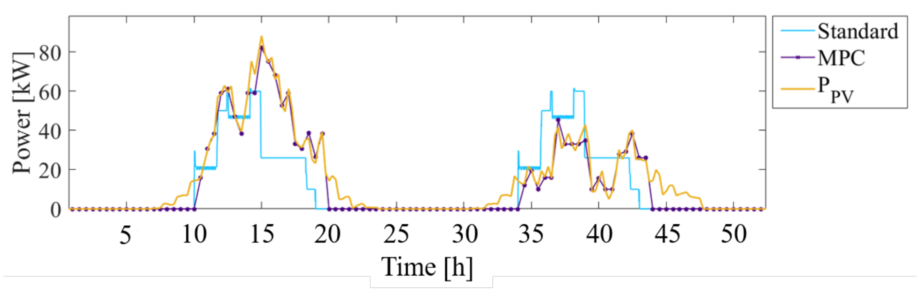

Figure 4 - Load and PV production profile for two typical summer days.

In this study a Li-Ion battery has been considered as stationary battery system. The battery has been mathematically modeled as in [46], but further details about the component degradation has been considered in the sizing optimization. The battery cycle lifetime has been estimated considering the degradation model proposed in [59]. The three-parameter model (see Equation 5) used for materials fatigue analysis has been fitted considering the lithium-ion battery experimental data available in literature [59], [60]:

$$N_{cycles}(DOD_{cycle}) = \frac{3320.8}{(DOD_{cycle} + 0.05)^{1.145}} \tag{5}$$

In Equation 5, N_{cycles} is the number of cycles before the end of life, (usually assumed to be at 80% remaining capacity) and DOD_{cycle} is the Depth of Discharge (DOD) of the cycle. The rainflow method [61] has been employed to decompose the battery DOD profile into micro cycles at different DOD, then Equation6 has been used to convert these cycles to the reference cycle at 80% and estimate the battery life (L_{cycle}) as:

$$L_{cycle} = \frac{N_{cycles}(80\%)}{\sum_{i=1}^{C}\left[\left(\frac{DOD_i + 0.05}{0.85}\right)^{1.145} \cdot R_i\right]} \tag{6}$$

where C is the total number of cycles in one year calculated through the rainflow method. The R_i coefficient is 0.5 for a half cycle or 1 for a full cycle. Also the calendar degradation, that is the gradual damage for batteries even when unused, should be taken into account. Thus, the BESS lifetime has been defined as the minimum between the cycle life (L_{cycle}) and the calendrical lifetime (assumed of 15 years).

The BESS is operated considering five variables: charging ($P_{BESSch,t}$) and discharging ($P_{BESSdch,t}$) power, charging ($\delta_{BESSch,t}$) and discharging ($\delta_{BESSdch,t}$) mode and State of Charge ($SOC_{BESS,t}$). Its dynamics is described by Equation 7:

$$SOC_{BESS,t} = SOC_{BESS,t-1} + \frac{P_{BESSch,t}}{C_{BESS}} \cdot \Delta t - \frac{P_{BESSdch,t}}{C_{BESS}} \cdot \Delta t \tag{7}$$

where C_{BESS} is the capacity of the battery and the efficiencies of the charging and discharging process are considered identical, namely 90%. For all the cases the initial BESS SOC is set equal to 90%. Due to the long time horizon considered for the simulation, (one year) different values for initial SOC have not been reported as the initial state of the battery has not a relevant impact on the final evaluation.

In order to evaluate the potential benefits offered by exploiting the logistic resources, the introduction of EVs in the carpentry's fleet has been considered. Two conventional vehicles are substituted by two electric vehicles with different battery capacity. Even if the use of EVs requires higher investment costs, its use might contribute to reduce the operating costs of the considered carpentry. Indeed, in the case in which the incentive time for feeding the grid has expired, the use of electric fleet might contribute to increase the self-consumption and therefor to supply at very low costs the required energy to the logistic sources.

It has been assumed that twice a week these EVs are used to transport the manufactured furniture to the shop center, and they remain connected to the grid when not travelling. In particular, one van is used for urban routes while the other for extra-urban routes. This assumption has been formulated after an interview with the carpentry operators. The urban trip is performed in 1.30 hours and the extra-urban trip in 2 hours. The time departure of the EV, as well as the delivery day, have been chosen randomly in the range between the 9 a.m. and 3 p.m. from Monday to Friday in order to take into account the uncertainty in time availability to recharge. The mean travel distance depicts real scenarios. Different works have been dealing with the minimization of the energy consumption under real traffic conditions for either PHEVs [62] or EVs [63]. Since the focus of the current study is on the factory side, mainly interested by charging related aspects, in this work the EVs battery discharging profiles have been defined considering an average energy consumption per km as declared by car manufacturers [64]. A conventional charging station, characterized by three different charging power levels (3.3 kW, 7.4kW and 11kW) has been used for the EVs charging process. Table 1 resumes the main features of the EVs.

Table 1 - EV Characteristic Parameter

Parameters	Units	Vehicle A/Vehicle B
Battery Capacity	[kWh]	91/170
Mean Travel Distance	[km]	40-50/140-150
Average Energy Consumption	[Wh/km]	325/850

Each EV is modelled through five variables: charging ($P_{EVch,t}$) and discharging ($P_{EVdch,t}$) power, charging ($\delta_{EVch,t}$) and discharging ($\delta_{EVdch,t}$) mode and State of Charge ($SOC_{EV,t}$). The EVs dynamics is described by Equation 8:

$$SOC_{EV,t} = SOC_{EV,t-1} + \frac{P_{EVch,t}}{C_{EV}} \cdot \eta_{ch} \cdot \Delta t - \frac{P_{EVdch,t}}{C_{EV}} \cdot \Delta t \tag{8}$$

where C_{EV} is the capacity of the EV battery and the charging efficiency process (η_{ch}) is assumed to be 90% and the discharging efficiency has been assumed to be already taken into account in the average energy consumption value.

Further constraints are imposed to avoid simultaneous charging and discharging state (Equation 9) and to limit the power value (Equation 10).

$$\delta_{BESSch,t} + \delta_{BESSdch,t} \leq 1 \tag{9}$$

$$\begin{aligned} P_{BESSch,t} &\leq P_{BESSch,MAX} \cdot \delta_{BESSch,t} \\ P_{BESSdch,t} &\leq P_{BESSdch,MAX} \cdot \delta_{BESSdch,t} \end{aligned} \tag{10}$$

By considering all the flexibility options, the objective function that the MILP algorithm aims at minimizing is the net energy exchanged with the grid over a given time horizon T (Equation 11):

$$min \sum_{t}^{T} (P_{feed,t} + P_{withdrawal,t}) \cdot \Delta t \tag{11}$$

such that

$$P_{load,t} + P_{feed,t} + P_{ch,t} = P_{withdral,t} + P_{dch,t} + P_{PV,t} \tag{12}$$

4. Optimal BESS Sizing Strategy

In order to find the optimal BESS sizing, different technical aspects should be considered. Indeed, the single objective of energy grid exchange minimization would result into the choice of installing the highest possible battery capacity. However, as showed in [65] this solution would be ineffective both from the technical and the economic point of view as the capacity exploitation and the marginal advantages are reduced increasing the BESS capacity. In [66] the optimal sizing problem is faced considering technical, economic, and environmental aspects, based on three optimization indicators: total annual costs, external electricity ratio and carbon dioxide emission value. A Rule Base Control (RBC) strategy is used to schedule the operation while a NSGA-II algorithm is implemented to optimally size the plant components. Differently, in this work, a MILP based framework is built to optimally plan the operation scheduling toward an increased flexibility of the system, while two objectives have been defined to carry out the multi-objective sizing optimization using a GA approach: the minimization of the annual energy exchanged with the grid (normalized with respect to the reference value obtained without BESS – Equation 13), and the minimization of the difference between $I_{size_{BESS}}$ and its technical optimal value ($I_{size_{BESS,OPT}}$ – Equation 14), where $I_{size,BESS}$ is an index describing the yearly exploitation of the battery, defined according to Equation 15. Using this technical parameter instead of economic- or technology-dependent parameters, allows the generalization of the approach regardless case-constraint input (geographic location of the industry, battery technology, etc.) still ensuring the proper use of the BESS. Indeed, targeting the optimal value of 1 ensure the battery to work averagely at its nominal capacity rate. This operative condition ($I_{size,BESS}$=1) could occur either if the battery works at high charge/discharge rate for a short period or it works constantly close to its nominal rate (1C). Thus, for the selected range of BESS capacities considered in the optimization, the average and the maximum charge and discharge C-rates have been evaluated during the whole period of observation. Both values are always within reasonable limits: between 1.2C for the smallest capacity and 0.2C for the biggest one confirming that the battery works close to its nominal charging/discharging rate and therefore that the value of $I_{size,BESS}$ equal to 1 is optimal.

$$Objective_1 = \frac{E_{grid}}{E_{grid_{REF}}} \tag{13}$$

$$Objective_2 = |I_{size_{BESS,OPT}} - I_{size_{BESS}}| \tag{14}$$

$$I_{size,BESS} = \frac{\sum_{i=1}^{k} E_{BESS_i}}{C_{BESS} \cdot k} \tag{15}$$

In Equation 15, $\sum_{i=1}^{k} E_{BESS_i}$ is the sum of the energy stored into the battery during a period k, that in this study is the number of days in a year.

According to Equations. 13 and 14, the two objectives require the knowledge of the energy fluxes among the system components and their dependence on the BESS size. However, during the design phase they are unknown since they depend on the control of the components themselves.

In [67] it is suggested to define the design problem according to a *leader-follower* approach, where the leader is the multi-objective battery sizing optimization and the follower is the optimal scheduling of the manufacturing process. More specifically, the following steps have been implemented in this paper:

1. Definition of the initial set of BESS capacity (C_{BESS}) candidates
2. Annual manufacturing scheduling and evaluation of annual E_{grid} and E_{BESS} for every C_{BESS} of the set
3. Definition of Objective$_1$ and Objective$_2$ as functions of C_{BESS} fitting the values found in 2
4. Evaluation through the multi-objective optimization of the optimal BESS capacity $C_{BESS,opt}$
5. The optimal value found in 4 is then added to the initial population and the optimization is performed again from point 2 upon convergence (with a tolerance equal to 1%).

Step 3 allows for a better and fast convergence of the algorithm as the space of solution with respect to a single objective has already been mapped. The sizing strategy is summarized in the flowchart shown in Figure 5. In particular, the multi-objective optimization is solved employing the Non-Sorted Genetic Algorithm (NSGA-II [68]). This is one of major heuristic multi-objective optimizer mainly based on a non-dominated sorting (NDS) and crowding distance sorting mechanisms to determine the Pareto Front. Such mechanisms ensure both the convergence and spreading of the population. In order to prevent a solution dependent on the algorithm's characteristic parameters, a sensitivity analysis has been performed, resulting in the values reported in Table 2. The GA has been solved using *gamultiobj* function implemented in Matlab, whereas the optimization scheduling formulated as a MILP algorithm has been solved by Gurobi. All the simulation have been run, for the whole horizon period of one year (52 weeks), using a Intel® Core™ i7-6500U CPU @2.50GHz.

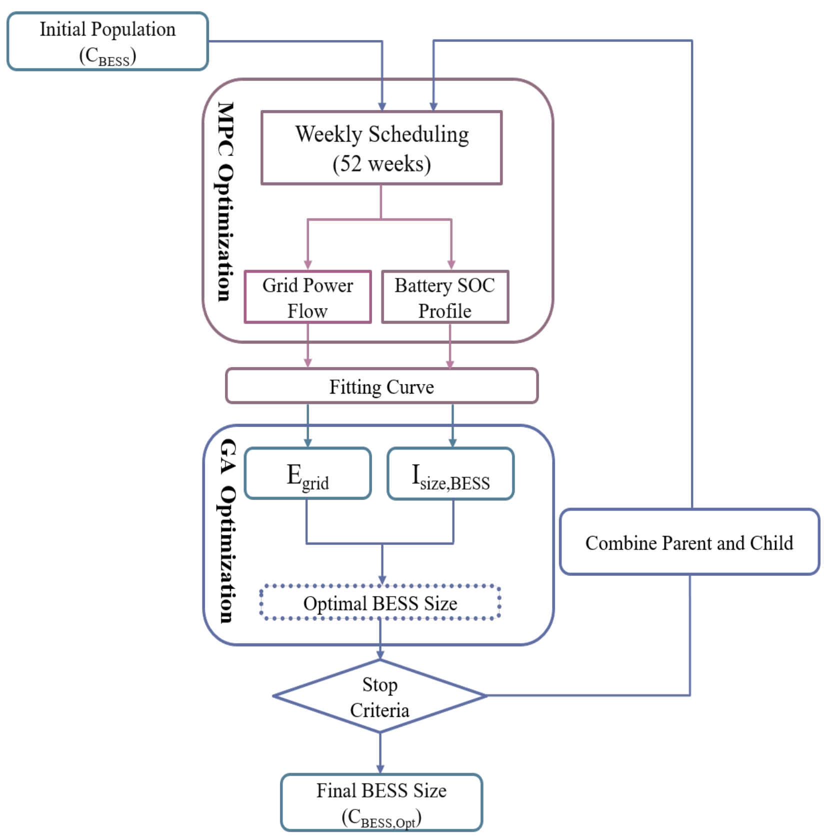

Figure 5 - Maximum, minimum and annual average C-rate of BESS charging and discharging for the case study with (red) and without (blue) EV

5. Results

In order to evaluate the goodness of the suggested approach and its contribution to operate the carpentry as net-zero energy factory, two scenarios have been considered. In the first one, the carpentry does not use the logistic resources for increasing its flexibility option. In the second one, the usage of electric vehicles has been taken in consideration. By doing it, two different time ranges have been considered: only working days or the whole week.

The outcomes of the multi-objective optimizations are shown in Figure 6 in form of Pareto fronts which analyses the considered system during one operating year. In particular, the result for the system configuration with EV is identified with rhombus and the one without EV with circles, while working days and whole week solutions are colored in red and blue, respectively.

Table 2 - Genetic Algorithm Configuration Parameter

Parameters	Values
Algorithm	NSGA II
Population Size	50
Selection	Tournament
Crossover function	Heuristic
Crossover ratio	0.8
Mutation function	Adaptive Feasible
Maximal generations	400
Pareto Fraction	0.35
Stall generations	100
Function tolerance	0.0001

In Figure 6a the Pareto set is represented onto the performance (objective) space: for any point of the Pareto, the value of $I_{size,BESS}$ is reported as a function of the energy grid exchange (in terms of percentage with respect a baseline case - a system without BESS). The Pareto front generated by the optimal BESS capacity values is the set of non-dominated solutions of the optimization process, meaning that among the element of the set there is no objective that can be improved without sacrificing the other. Thus, the shape of this front can provide general guidelines to the factory operator about how changes in design variables would influence the performance of the BESS. In Figure 6b, instead, the Pareto points are represented onto a single objective space (the energy grid exchange objective) and the different performance in reaching the NZEF goal between the four analyzed cases is more evident.

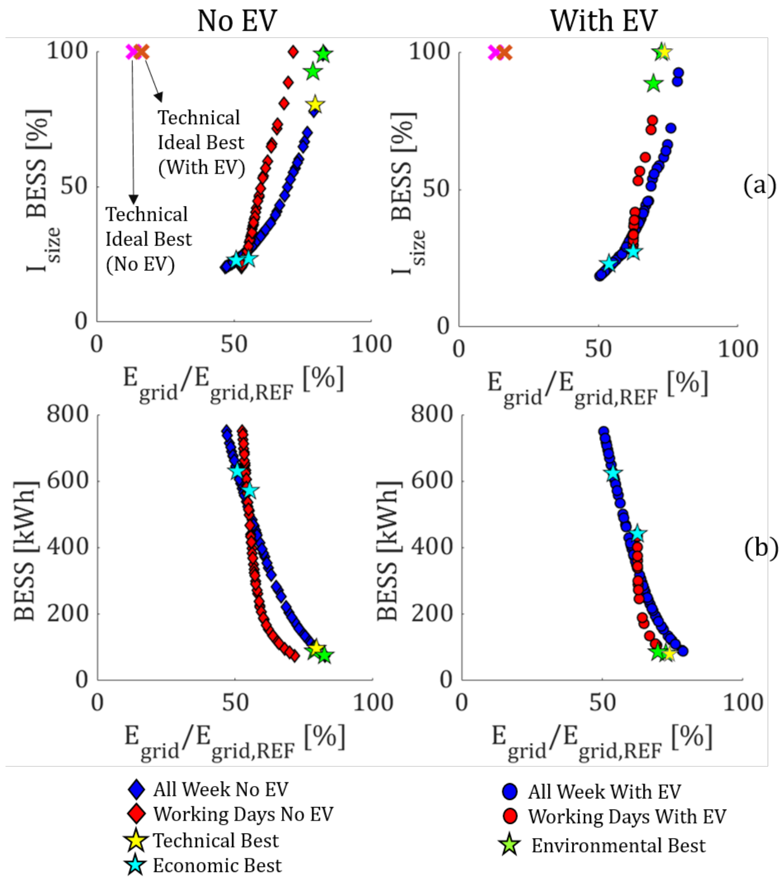

Figure 6 - (a) Pareto Fronts for the configuration without EV (rumble) and with EV (circles), considering all the week (blue) and only the working days (red); (b) optimal BESS sizes of the Pareto fronts as a function of the energy grid exchange reduction (technical best : yellow stars; economic best: light blue stars; environmental best: green stars).

Looking at the two Pareto fronts in blue in Figure 6a, a difference in the fronts slopes can be noticed close to the value of 300kWh of BESS capacity. This reflects the EVs capability in giving more room for the reduction of the energy exchanged with the grid. Indeed, for the smaller battery capacity cases (right side of the Pareto curve), EVs are programmed to be recharged during the weekend and the surplus energy (that would have been sold to the grid otherwise) decreases. On contrary, energy absorption of EV batteries trades off higher BESS sizes, which in turn, appear less effective.

This is particularly evident, for example, for cloudy weekends as the one shown in Figure 7. In this case, due to the limited amount of energy available from PV, the battery starts the weekend with 30% of SOC and due to the contemporary requests of energy for charging the stationary BESS and the EVs the final stationary BESS SOC is not fully charged at the end of the weekend.

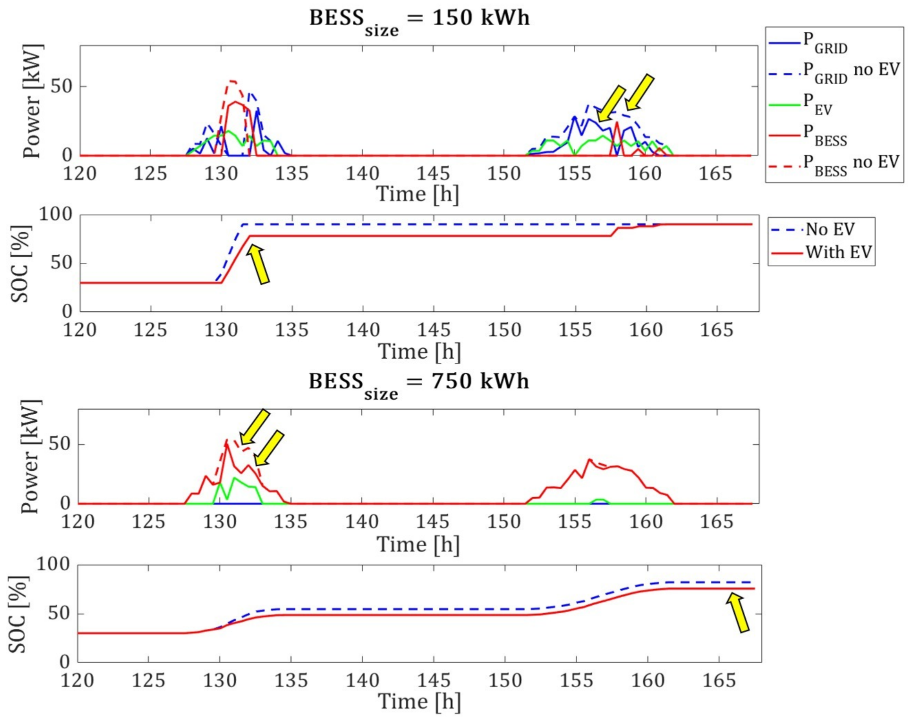

Figure 7 – Power profiles of grid, EV and battery as well battery SOC for two sizes of BESS in a cloudy weekend.

This negative effect due to the power absorbed by EVs is even more evident whenever only working days are considered. Indeed, the decreased slope of the energy grid exchanged curve as a function of BESS capacity, indicates a more evident saturation effect with increased BESS capacity.

Among all the optimal solutions within the Pareto front, the battery capacity choice involves the decision maker preferences. In particular, the choosing criteria should be independent on the two objectives, as the points of the Pareto frons are all optima, as explained before. In this study, three main targets have been considered: technical, economic or environmental.

The best technical choice can be defined by considering the point closer (i.e. with the shortest distance D_{BESS}) to the ideal optimal technical point with D_{BESS} defined as:

$$D_{BESS} = \sqrt{\alpha_1 \cdot (\frac{E_{grid,id} - E_{grid}}{E_{grid_{REF}}})^2 + \alpha_2 \cdot (I_{size,BESSid} - I_{size,BESS})^2} \quad (16)$$

where α_1 and α_2 are the weights associated to energy grid exchange and BESS capacity exploitation respectively, $E_{grid,id}$ is the minimum possible value of energy exchanged with the grid by considering all the PV energy self-consumed by the factory ($|E_{PV} - E_{LOAD}|$) and $I_{size,BESSid}$ is equal to 1. Assuming that the two objectives have equal importance, α_1 and α_2 are set equal to 1, and D_{BESS} is than the length of the line connecting any point of the Pareto Front in Figure 5a from either the magenta or the orange cross. The points with minimum distance (marked with yellow stars) represent the best technical sizes.

The economic optimal choice, instead, could be found evaluating the annual economic savings achievable by installing a certain BESS capacity. In particular, in this study, economic savings have been defined as the difference in the annual energy bill between two systems (see Table 3 for more details), with and without the BESS. The optimal economic points (Ciano stars in Fig 6) have then been identified corresponding to the BESS capacity where the marginal gain starts to decrease remarkably (i.e. where the slope of the Annual Saving curve is decreased in Figure 8).

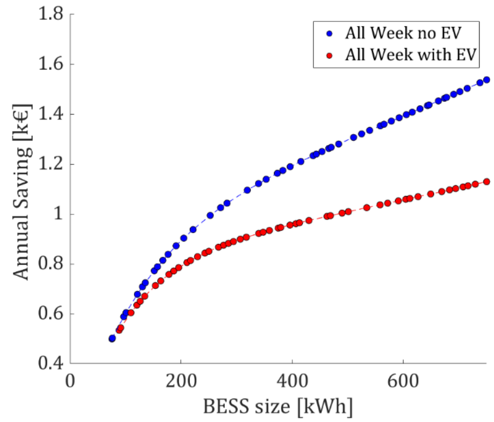

Figure 8 - Annual saving in the electric bill for the two system configurations: without EV (blue) and with EV (red)

When the environmental aspect is taken into account, the optimal BESS capacity would be the one ensuring the highest amount of CO_2 emissions saved over the system lifetime (here assumed as 15 years). To evaluate the system carbon footprint, Global Warming Potential (GWP) factors for both energies taken from the grid and battery production/recycling processes have been considered. In particular, the total CO_2 emissions saved have been calculated with Equations 17 and 18, with and without EVs, respectively:

$$Emissions = (E_{withdrawn} \cdot 15) \cdot GWP_{GRID} + e_{travel} \cdot 15 - BESS_{size} \cdot GWP_{BESS} \cdot \frac{15}{life_{BESS}} \quad (17)$$

$$Emissions = (E_{withdrawn} \cdot 15) \cdot GWP_{GRID} - BESS_{size} \cdot GWP_{BESS} \cdot \frac{15}{life_{BESS}} \quad (18)$$

where e_{travel} represents the total emissions of a diesel vehicle used for the transportation of goods from the factory in place of EVs, $C_{EV1}$and C_{EV2} are the EV battery capacities , GWP_{GRID} and GWP_{BESS} are the Global Warming Potential values for the grid and a representative Li-Ion battery. The trend of avoided emissions with BESS capacity is shown in Figure 8.

The two curves are discontinuous at the point of BESS size where the number of battery replacement changes. It could be noticed that pursuing the environmental goal leads to choose the smallest battery capacity (green star symbols in Figure 6) since, beyond a certain sizing, the environmental impact related to the batteries life-cycle overcomes the savings due to the avoided fuel and grid energy purchased. However, the best techno-environmental compromise would be represented by a neutral carbon footprint system (horizontal dashed line in Figure 9). According to this requirement, the optimal BESS size moves towards higher capacities: around 440kWh and 360kWh for a system without and with EV, respectively.

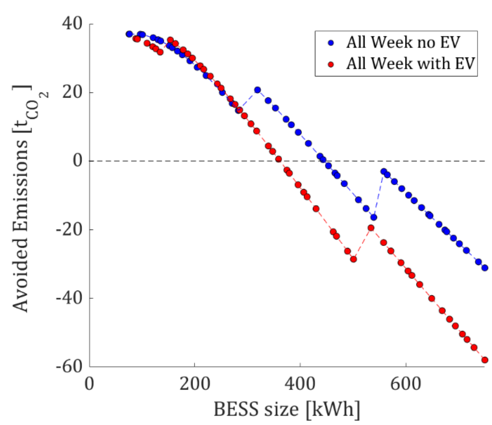

Figure 9 - Saved CO2 emission along the system life for the two system configurations: without EV (blue) and with EV (red)

Table 3 reports the values used to calculate the economic and the environmental best BESS sizes [60], [69]–[71], while Table 4 and 5 summarizes the results obtained in terms of optimal BESS sizing for each of the user's goal and the corresponding values of annual economic and emission savings [72].

Table 3 - Economic and environmental parameters

Component	Cost	Global Warming Potential (GWP)	Emission Factor	
	Withdrawal [€/kWh]	[kgCO$_2$ /kWh[1]]	[kgCO$_2$ /kWh[2]]	[kgCO$_2$/km]
GRID	0.15		0.658	
BESS		112.1		
EV1				0.213
EV2				0.186

[1] kWh installed
[2] kWh consumed

Table 4 - BESS optimal Capacity (Power [60])

Case Study		Sizes (Capacity in kWh, Power in kW)		
		Technical	Economical	Environmental
No EV	All Week	100 (106)	630 (150)	75 (80)
	Working Days	85 (90)	620 (150)	85 (90)
With EV	All Week	90 (95)	570 (120)	90 (95)
	Working Days	80 (85)	440 (120)	80 (85)

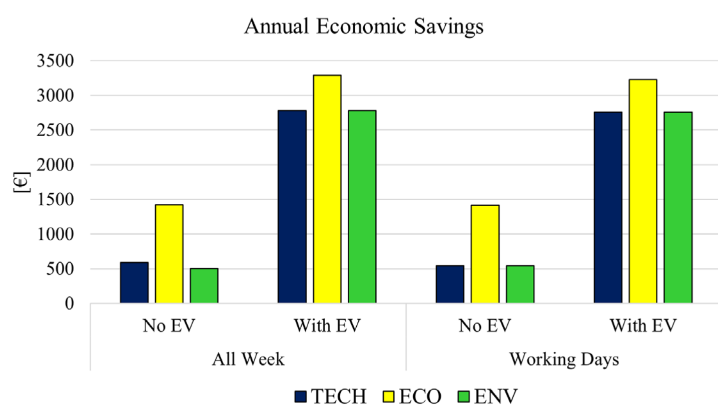

(a)

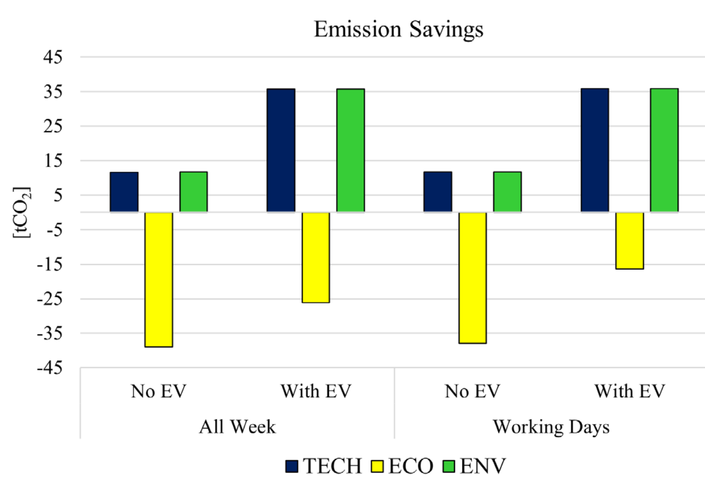

(b)

Figure 10 - Annual Economic Savings and Emission Savings with the optimal BESS capacities

Table 4 shows that targeting three different goals separately lead to completely different BESS size choice, highlighting the importance of taking a global perspective in order to consider all the trades-off present in the design process.

It could be noted in Figure 10 that EVs usage helps to increase significantly the annual monetary savings from 128% up to 406%. A strong reduction till 67% in the carbon footprint could be observed as well. These differences are extremely high for small battery capacities (technical and environmental BESS choices) as it increases the relative advantage in terms of both the economic and CO_2 emission savings due to the reduction in fuel consumption.

A final consideration can be stated on the role of EVs in affecting the self-consumption of the renewable energy produced. A self-consumption index (I_{SC}) is defined as the fraction of the energy produced by PV that is used to meet the loads (Equation 19) and it has been represented in Figure 11. It can be observed that EVs increase around 5% the self-consumption of the system for all the BESS sizes. In particular, an increase up to 11% is observed for the environmental best design solution. This positive effect is due to the optimal management of the surplus energy produced.

$$I_{SC} = \frac{E_{PV} - E_{GRID}}{E_{PV}} \tag{19}$$

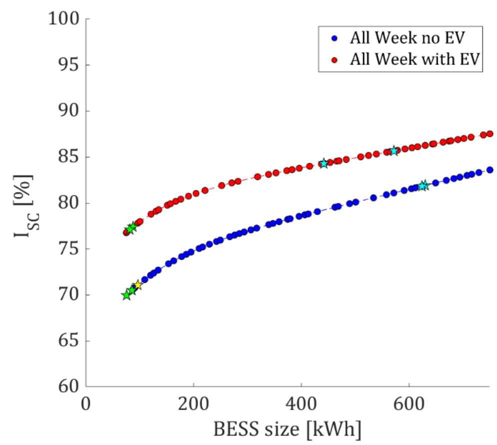

Figure 11 - Self Consumption Index as a function of the BESS capacity with and without EV (technical best: yellow stars; economic best: light blue stars; environmental best: green stars) configurations: without EV (blue) and with EV (red).

Conclusions

This work aimed at highlighting benefits and criticalities of the optimal sizing of a Battery Energy Storage System (BESS) for a manufacturing enterprise, targeting the “Net Zero Energy Factory” (NZEF) goal. Annual simulations for manufacturing production planning and energy management have been performed with a Model Predictive Control strategy. A Genetic Algorithm has been used to define the optimal Pareto front in terms of energy grid exchange reduction and optimal exploitation of the battery capacity. Then, according to the decision maker preferences, technical, economic and environmental optimal battery capacities have been defined and commented on. The influence of the integration of Electric Vehicles on the system design and operation have been assessed.

The main conclusions of the paper can be listed as follows:

- A saturation effect on energy grid exchange reduction with BESS capacity increase could be observed, especially when only working days are considered: a maximum reduction of 53% has been achieved for the BESS range analyzed;
- The presence of EVs is beneficial when a small battery size is chosen as it helps to reduce the energy sold to the grid during the weekend, increasing of about 5% the I_{SC} of the system;
- The integration of EVs moves the point of optimal BESS size towards lower values, both when the economic and the environmental goals are targeted;
- EVs use helps to increase the annual monetary savings till 406% and the carbon footprint till 67% since the primary energy consumption (electricity and fuel) of the system is overall reduced.

From the above considerations, it emerges that, when aiming at a “Net Zero Energy Factory”, it is not possible to consider in the design process only the energetic perspective. Indeed, economic and environmental aspects should be evaluated to make a globally optimal choice. The case study presented has highlighted some intrinsic limitation for the factories operating only during the weekdays due to the PV overproduction during the weekend. Thus, considering only the NZEF goal would lead to oversize the BESS capacities. However, accounting for economic, environmental and technical aspects the BESS design significantly changes moving towards lower values. Further advantages could be obtained with the integration of a different energy vector, as for example hydrogen. Thus, future works will consider a more complex system introducing hydrogen fueled vehicles and will be aimed to analyze the benefits and the challenges arising from the combined optimal sizing of both the electric energy and the hydrogen storage systems. Besides, the possibility to supply the load through a hybrid AC/DC system will be further investigated. Indeed, if the voltage of the machines and of the energy storage systems are controlled by smart transformers, the flexibility degree of a NZEF could be further increased [73].

Acknowledgment

This project has received funding in the framework of the joint programming initiative ERA-Net Smart Energy Systems' focus initiatives Smart Grids Plus and Integrated, Regional Energy Systems, with support from the European Union's Horizon 2020 research and innovation program under grant agreements No 646039 and 775970.

References

[1] "Energiewende." .
[2] "Bundesministerium für wirtschaft und energie," 2019.
[3] R. C. Dugan, J. A. Taylor, and D. Montenegro, "Energy storage modeling for distribution planning," *IEEE Trans. Ind. Appl.*, vol. 53, no. 2, pp. 954–962, 2017, doi: 10.1109/TIA.2016.2639455.
[4] T. M. Gür, "Review of electrical energy storage technologies, materials and systems: Challenges and prospects for large-scale grid storage," *Energy Environ. Sci.*, vol. 11, no. 10, pp. 2696–2767, 2018, doi: 10.1039/c8ee01419a.
[5] H.-W. Sinn, "Buffering volatility: A study on the limits of Germany's energy revolution," *Eur. Econ. Rev.*, vol. 99, pp. 130–150, 2017, doi: https://doi.org/10.1016/j.euroecorev.2017.05.007.
[6] M. Ross, C. Abbey, F. Bouffard, and G. Joós, "Multiobjective optimization dispatch for microgrids with a high penetration of renewable generation," *IEEE Trans. Sustain. Energy*, vol. 6, no. 4, pp. 1306–1314, 2015, doi: 10.1109/TSTE.2015.2428676.
[7] B. Wang, C. Zhang, and Z. Y. Dong, "Interval Optimization Based Coordination of Demand Response and Battery Energy Storage System Considering SOC Management in a Microgrid," *IEEE Trans. Sustain. Energy*, vol. 11, no. 4, pp. 2922–2931, 2020, doi: 10.1109/tste.2020.2982205.
[8] S. Kotra and M. K. Mishra, "Design and stability analysis of DC microgrid with hybrid energy storage system," *IEEE Trans. Sustain. Energy*, vol. 10, no. 3, pp. 1603–1612, 2019, doi: 10.1109/TSTE.2019.2891255.
[9] "Demand Response in Industrial Production (DRIP)." .
[10] "IndustRE, 'Using the flexibility potential in energy intensive industries to facilitate further grid integration of variable renewable energy sources.'" .
[11] Y. Lu, S. Wang, and K. Shan, "Design optimization and optimal control of grid-connected and standalone nearly/net zero energy buildings," *Appl. Energy*, vol. 155, pp. 463–477, 2015, doi: https://doi.org/10.1016/j.apenergy.2015.06.007.
[12] B. Verbruggen and J. Driesen, "Grid impact indicators for active building simulations," *IEEE Trans. Sustain. Energy*, vol. 6, no. 1, pp. 43–50, 2015, doi: 10.1109/TSTE.2014.2357475.
[13] M. Ferraro, F. Sergi, V. Antonucci, F. Guarino, G. Tumminia, and M. Cellura, "Load match and grid interaction optimization of a net zero energy building through electricity storage: An Italian case-study," *EEEIC 2016 - Int. Conf. Environ. Electr. Eng.*, 2016, doi: 10.1109/EEEIC.2016.7555812.
[14] F. Liberati, A. Di Giorgio, A. Giuseppi, A. Pietrabissa, E. Habib, and L. Martirano, "Joint Model Predictive Control of Electric and Heating Resources in a Smart Building," *IEEE Trans. Ind. Appl.*, vol. 55, no. 6, pp. 7015–7027, 2019, doi: 10.1109/TIA.2019.2932954.
[15] X. Li, A. Lin, C.-H. Young, Y. Dai, and C.-H. Wang, "Energetic and economic evaluation of hybrid solar energy systems in a residential net-zero energy building," *Appl. Energy*, vol. 254, p. 113709, 2019, doi: https://doi.org/10.1016/j.apenergy.2019.113709.
[16] J. Salpakari, T. Rasku, J. Lindgren, and P. D. Lund, "Flexibility of electric vehicles and space heating in net zero energy houses: an optimal control model with thermal dynamics and battery degradation," *Appl. Energy*, vol. 190, pp. 800–812, 2017, doi: https://doi.org/10.1016/j.apenergy.2017.01.005.
[17] K. F. Fong and C. K. Lee, "Towards net zero energy design for low-rise residential buildings in subtropical Hong Kong," *Appl. Energy*, vol. 93, pp. 686–694, 2012, doi: https://doi.org/10.1016/j.apenergy.2012.01.006.
[18] H. Yu, S. Niu, Y. Zhang, and L. Jian, "An integrated and reconfigurable hybrid AC/DC microgrid architecture with autonomous power flow control for nearly/net zero energy buildings," *Appl. Energy*, vol. 263, p. 114610, 2020, doi: https://doi.org/10.1016/j.apenergy.2020.114610.
[19] P. Lombardi, P. Sokolnikova, B. Arendarski, R. Franke, A. Hoepfner, and P. Komarnicki, "Multi-Criteria Planning Tool for a Net Zero Energy Village," *Proc. - 2018 IEEE Int. Conf. Environ. Electr. Eng. 2018 IEEE Ind. Commer. Power Syst. Eur. EEEIC/I CPS Eur. 2018*, 2018, doi: 10.1109/EEEIC.2018.8493651.
[20] P. Sokolnikova *et al.*, "Net-zero multi-energy systems for Siberian rural communities: A methodology to size thermal and electric storage units," *Renew. Energy*, vol. 155, pp. 979–989, 2020, doi: 10.1016/j.renene.2020.03.011.
[21] "Tesla Gigafactory." .
[22] "Mitsubishi Electric Facility Receives Net Zero Energy Building Certification." .

[23] C. Marnay *et al.*, "Microgrid evolution roadmap," *Proc. - 2015 Int. Symp. Smart Electr. Distrib. Syst. Technol. EDST 2015*, no. August 2010, pp. 139–144, 2015, doi: 10.1109/SEDST.2015.7315197.
[24] M. W. Khan, J. Wang, and L. Xiong, "Optimal energy scheduling strategy for multi-energy generation grid using multi-agent systems," *Int. J. Electr. Power Energy Syst.*, vol. 124, p. 106400, Jan. 2021, doi: 10.1016/J.IJEPES.2020.106400.
[25] H. Golmohamadi, R. Keypour, B. Bak-Jensen, and J. R. Pillai, "A multi-agent based optimization of residential and industrial demand response aggregators," *Int. J. Electr. Power Energy Syst.*, vol. 107, pp. 472–485, May 2019, doi: 10.1016/J.IJEPES.2018.12.020.
[26] J. P. Usuga Cadavid, S. Lamouri, B. Grabot, R. Pellerin, and A. Fortin, "Machine learning applied in production planning and control: a state-of-the-art in the era of industry 4.0," *J. Intell. Manuf.*, vol. 31, no. 6, pp. 1531–1558, 2020, doi: 10.1007/s10845-019-01531-7.
[27] D. Ramin, S. Spinelli, and A. Brusaferri, "Demand-side management via optimal production scheduling in power-intensive industries: The case of metal casting process," *Appl. Energy*, vol. 225, pp. 622–636, 2018, doi: https://doi.org/10.1016/j.apenergy.2018.03.084.
[28] D. L. Summerbell, D. Khripko, C. Barlow, and J. Hesselbach, "Cost and carbon reductions from industrial demand-side management: Study of potential savings at a cement plant," *Appl. Energy*, vol. 197, pp. 100–113, 2017, doi: https://doi.org/10.1016/j.apenergy.2017.03.083.
[29] M. Manana *et al.*, "Increase of capacity in electric arc-furnace steel mill factories by means of a demand-side management strategy and ampacity techniques," *Int. J. Electr. Power Energy Syst.*, vol. 124, p. 106337, Jan. 2021, doi: 10.1016/J.IJEPES.2020.106337.
[30] M. Choobineh and S. Mohagheghi, "Optimal Energy Management in an Industrial Plant Using On-Site Generation and Demand Scheduling," *IEEE Trans. Ind. Appl.*, vol. 52, no. 3, pp. 1945–1952, 2016, doi: 10.1109/TIA.2015.2511094.
[31] L. Ferrari *et al.*, "Development of an optimization algorithm for the energy management of an industrial Smart User," *Appl. Energy*, vol. 208, pp. 1468–1486, 2017, doi: https://doi.org/10.1016/j.apenergy.2017.09.005.
[32] H. Zhang, J. Cai, K. Fang, F. Zhao, and J. W. Sutherland, "Operational optimization of a grid-connected factory with onsite photovoltaic and battery storage systems," *Appl. Energy*, vol. 205, pp. 1538–1547, 2017, doi: https://doi.org/10.1016/j.apenergy.2017.08.140.
[33] M. Yu, R. Lu, and S. H. Hong, "A real-time decision model for industrial load management in a smart grid," *Appl. Energy*, vol. 183, pp. 1488–1497, 2016, doi: https://doi.org/10.1016/j.apenergy.2016.09.021.
[34] Y. Wang, C. Chen, Y. Tao, Z. Wen, B. Chen, and H. Zhang, "A many-objective optimization of industrial environmental management using NSGA-III: A case of China's iron and steel industry," *Appl. Energy*, vol. 242, pp. 46–56, 2019, doi: https://doi.org/10.1016/j.apenergy.2019.03.048.
[35] M. Richter *et al.*, "A vision for energy decarbonization: Planning sustainable tertiary sites as net-zero energy systems," *Energies*, vol. 14, no. 17, 2021, doi: 10.3390/en14175577.
[36] Z. S. P. Komarnicki, P. Lombardi, *Electric Energy Storage Systems: Flexibility Options for Smart Grids*. Springer, 2017.
[37] T. K. Chau, S. S. Yu, T. Fernando, and H. H. C. Iu, "Demand-Side Regulation Provision From Industrial Loads Integrated With Solar PV Panels and Energy Storage System for Ancillary Services," *IEEE Trans. Ind. Informatics*, vol. 14, no. 11, pp. 5038–5049, 2018, doi: 10.1109/TII.2017.2782244.
[38] F. Reda and Z. Fatima, "Northern European nearly zero energy building concepts for apartment buildings using integrated solar technologies and dynamic occupancy profile: Focus on Finland and other Northern European countries," *Appl. Energy*, vol. 237, pp. 598–617, 2019, doi: https://doi.org/10.1016/j.apenergy.2019.01.029.
[39] X. Wang, N. H. El-Farra, and A. Palazoglu, "Optimal scheduling of demand responsive industrial production with hybrid renewable energy systems," *Renew. Energy*, vol. 100, pp. 53–64, 2017, doi: https://doi.org/10.1016/j.renene.2016.05.051.
[40] A. A. Eladl, M. I. El-Afifi, M. A. Saeed, and M. M. El-Saadawi, "Optimal operation of energy hubs integrated with renewable energy sources and storage devices considering CO2 emissions," *Int. J. Electr. Power Energy Syst.*, vol. 117, p. 105719, May 2020, doi: 10.1016/J.IJEPES.2019.105719.
[41] Z. L. Hurwitz, Y. Dubief, and M. Almassalkhi, "Economic efficiency and carbon emissions in multi-energy systems with flexible buildings," *Int. J. Electr. Power Energy Syst.*, vol. 123, p. 106114, Dec. 2020, doi: 10.1016/J.IJEPES.2020.106114.
[42] J. M. Alemany, B. Arendarski, P. Lombardi, and P. Komarnicki, "Accentuating the renewable energy exploitation: Evaluation of flexibility options," *Int. J. Electr. Power Energy Syst.*, vol. 102, pp. 131–151, 2018, doi: https://doi.org/10.1016/j.ijepes.2018.04.023.
[43] P. Lombardi, B. Arendarski, P. Komarnicki, M. Santarelli, A. Pantaleo, and M. Liserre, "Exploitation of flexbility within net-zero energy factories. A study case for a german carpentry works," *2019 IEEE Int. Conf. Environ. Electr. Eng. 2019 IEEE Ind. Commer. Power Syst. Eur. (EEEIC / I&CPS Eur. Environ. Electr. Eng. 2019 IEEE Ind. Commer. Power Syst. E*.
[44] L. Bartolucci, S. Cordiner, V. Mulone, and S. Pasquale, "Hydrogen based Multi Energy Systems : Assessment of the marginal utility of increasing hydrogen penetration on system performances," *Int. J. Hydrogen Energy*, no. xxxx, 2021, doi: 10.1016/j.ijhydene.2021.09.108.
[45] C. Caro-Ruiz *et al.*, "Coordination of optimal sizing of energy storage systems and production buffer stocks in a net zero

energy factory," *Appl. Energy*, vol. 238, pp. 851–862, 2019, doi: https://doi.org/10.1016/j.apenergy.2019.01.125.
[46] L. Bartolucci *et al.*, "MPC-based Electric Energy Storage Sizing for a Net Zero Energy Factory," in *2019 IEEE International Conference on Environment and Electrical Engineering and 2019 IEEE Industrial and Commercial Power Systems Europe (EEEIC / I&CPS Europe)*, Jun. 2019, pp. 1–6, doi: 10.1109/EEEIC.2019.8783469.
[47] A. L. Facci, V. K. Krastev, G. Falcucci, and S. Ubertini, "Smart integration of photovoltaic production, heat pump and thermal energy storage in residential applications," *Sol. Energy*, vol. 192, no. December 2017, pp. 133–143, 2019, doi: 10.1016/j.solener.2018.06.017.
[48] A. Pham, T. Jin, C. Novoa, and J. Qin, "A multi-site production and microgrid planning model for net-zero energy operations," *Int. J. Prod. Econ.*, vol. 218, no. April, pp. 260–274, 2019, doi: 10.1016/j.ijpe.2019.04.036.
[49] M. Casini, G. G. Zanvettor, M. Kovjanic, and A. Vicino, "Optimal energy management and control of an industrial microgrid with plug-in electric vehicles," *IEEE Access*, vol. 7, p. 101729, 2019, doi: 10.1109/ACCESS.2019.2930274.
[50] S. Y. Derakhshandeh, A. Ghiasian, and M. A. S. Masoumm, "A New Time-Decoupled Framework for PEVs Charging and Scheduling in Industrial Microgrids," *IEEE Trans. Smart Grid*, vol. 10, no. 1, pp. 568–577, 2019, doi: 10.1109/TSG.2017.2748970.
[51] L. Bartolucci, S. Cordiner, V. Mulone, and M. Santarelli, "Ancillary services provided by hybrid residential renewable energy systems through thermal and electrochemical storage systems," *Energies*, vol. 12, no. 12, 2019, doi: 10.3390/en12122429.
[52] Y. Xie, L. Liu, Q. Wu, and Q. Zhou, "Robust model predictive control based voltage regulation method for a distribution system with renewable energy sources and energy storage systems," *Int. J. Electr. Power Energy Syst.*, vol. 118, p. 105749, Jun. 2020, doi: 10.1016/J.IJEPES.2019.105749.
[53] A. Moradmand, M. Dorostian, and B. Shafai, "Energy scheduling for residential distributed energy resources with uncertainties using model-based predictive control," *Int. J. Electr. Power Energy Syst.*, vol. 132, p. 107074, Nov. 2021, doi: 10.1016/J.IJEPES.2021.107074.
[54] L. Bartolucci, S. Cordiner, V. Mulone, V. Rocco, and J. L. Rossi, "Hybrid renewable energy systems for renewable integration in microgrids: Influence of sizing on performance," *Energy*, vol. 152, pp. 744–758, 2018, doi: 10.1016/j.energy.2018.03.165.
[55] L. Bartolucci, S. Cordiner, V. Mulone, V. Rocco, and J. L. Rossi, "Renewable source penetration and microgrids: Effects of MILP – Based control strategies," *Energy*, vol. 152, pp. 416–426, 2018, doi: 10.1016/j.energy.2018.03.145.
[56] A. Bolzoni, A. Parisio, R. Todd, and A. Forsyth, "Model Predictive Control for optimizing the flexibility of sustainable energy assets: An experimental case study," *Int. J. Electr. Power Energy Syst.*, vol. 129, p. 106822, Jul. 2021, doi: 10.1016/J.IJEPES.2021.106822.
[57] S. Choi and S. W. Min, "Optimal scheduling and operation of the ESS for prosumer market environment in grid-connected industrial complex," *2017 IEEE Ind. Appl. Soc. Annu. Meet. IAS 2017*, vol. 2017-Janua, no. 3, pp. 1–7, 2017, doi: 10.1109/IAS.2017.8101727.
[58] E. Bernardi, M. M. Morato, P. R. C. Mendes, J. E. Normey-Rico, and E. J. Adam, "Fault-tolerant energy management for an industrial microgrid: A compact optimization method," *Int. J. Electr. Power Energy Syst.*, vol. 124, p. 106342, Jan. 2021, doi: 10.1016/J.IJEPES.2020.106342.
[59] Y. Zhang, A. Lundblad, P. E. Campana, F. Benavente, and J. Yan, "Battery sizing and rule-based operation of grid-connected photovoltaic-battery system: A case study in Sweden," *Energy Convers. Manag.*, vol. 133, pp. 249–263, 2017, doi: https://doi.org/10.1016/j.enconman.2016.11.060.
[60] M. Baumann, J. F. Peters, M. Weil, and A. Grunwald, "CO2 Footprint and Life-Cycle Costs of Electrochemical Energy Storage for Stationary Grid Applications," *Energy Technol.*, vol. 5, no. 7, pp. 1071–1083, 2017, doi: 10.1002/ente.201600622.
[61] I. Rychlik, "A new definition of the rainflow cycle counting method," *Int. J. Fatigue*, vol. 9, no. 2, pp. 119–121, 1987, doi: https://doi.org/10.1016/0142-1123(87)90054-5.
[62] M. Montazeri-Gh and M. Mahmoodi-K, "Optimized predictive energy management of plug-in hybrid electric vehicle based on traffic condition," *J. Clean. Prod.*, vol. 139, pp. 935–948, Dec. 2016, doi: 10.1016/J.JCLEPRO.2016.07.203.
[63] J. D. Valladolid, D. Patino, G. Gruosso, C. A. Correa-Flórez, J. Vuelvas, and F. Espinoza, "A novel energy-efficiency optimization approach based on driving patterns styles and experimental tests for electric vehicles," *Electron.*, vol. 10, no. 10, pp. 1–21, 2021, doi: 10.3390/electronics10101199.
[64] "Electric Trucks and Vans." .
[65] G. Mulder, F. De Ridder, and D. Six, "Electricity storage for grid-connected household dwellings with PV panels," *Sol. Energy*, vol. 84, no. 7, pp. 1284–1293, 2010, doi: https://doi.org/10.1016/j.solener.2010.04.005.
[66] Y. Wang *et al.*, "Optimal design of integrated energy system considering economics, autonomy and carbon emissions," *J. Clean. Prod.*, vol. 225, pp. 563–578, 2019, doi: 10.1016/j.jclepro.2019.03.025.
[67] B. Li, R. Roche, and A. Miraoui, "Microgrid sizing with combined evolutionary algorithm and MILP unit commitment," *Appl. Energy*, vol. 188, pp. 547–562, 2017, doi: 10.1016/j.apenergy.2016.12.038.
[68] K. Deb, A. Pratap, S. Agarwal, and T. Meyarivan, "A fast and elitist multiobjective genetic algorithm: NSGA-II," *IEEE Trans. Evol. Comput.*, vol. 6, no. 2, pp. 182–197, 2002, doi: 10.1109/4235.996017.
[69] "No Title." .

[70] "MAN launches first all-electric production model." .
[71] K. Grave *et al.*, "Electricity Costs of Energy Intensive Industries: An International Comparison," *Frauenhofer & Ecofys*, no. 2015, pp. 1–84, 2015.
[72] "Energy Storage Solutions for business." .
[73] M. L. P. Lombardi, B. Arendarski, G. De Carne, C. Wenge, P. Komarnici, "Smart Transformer Use in Net-Zero Energy Factories."